https://doi.org/10.1093/plphys/kiac295 PLANT PHYSIOLOGY 2022: 190: 532–547

Plant Physiology®

Research Article

WRKY63 transcriptional activation of *COOLAIR* and *COLDAIR* regulates vernalization-induced flowering

Fu-Yu Hung [1,†] Yuan-Hsin Shih [1,†] Pei-Yu Lin [1] Yun-Ru Feng [1] Chenlong Li [2] and Keqiang Wu [1,*]

1 Institute of Plant Biology, National Taiwan University, Taipei 10617, Taiwan
2 State Key Laboratory of Biocontrol and Guangdong Key Laboratory of Plant Resource, School of Life Sciences, Sun Yat-sen University, Guangzhou 510275, China

*Author for correspondence: kewu@ntu.edu.tw
†These authors contributed equally

F.-Y.H., Y.-H.S., and K.W. designed research. Y.-H.S., P.-Y.L., F.-Y.H., Y.-R.F., and C.L. performed research. F.-Y.H., Y.-H.S., P.-Y.L., C.L., and K.W. analyzed data. F.-Y.H., Y.-H.S., P.-Y.L., and K.W. wrote the article.
The author responsible for distribution of materials integral to the findings presented in this article in accordance with the policy described in the Instructions for Authors (https://academic.oup.com/plphys/pages/general-instructions) is: Keqiang Wu (kewu@ntu.edu.tw).

Abstract

Arabidopsis (*Arabidopsis thaliana*) FLOWERING LOCUS C (FLC) acts as a key flowering regulator by repressing the expression of the floral integrator *FLOWERING LOCUS T* (*FT*). Prolonged exposure to cold (vernalization) induces flowering by reducing *FLC* expression. The long noncoding RNAs (lncRNAs) *COOLAIR* and *COLDAIR*, which are transcribed from the 3′ end and the first intron of *FLC*, respectively, are important for *FLC* repression under vernalization. However, the molecular mechanism of how *COOLAIR* and *COLDAIR* are transcriptionally activated remains elusive. In this study, we found that the group-III WRKY transcription factor WRKY63 can directly activate *FLC*. *wrky63* mutant plants display an early flowering phenotype and are insensitive to vernalization. Interestingly, we found that WRKY63 can activate the expression of *COOLAIR* and *COLDAIR* by binding to their promoters.WRKY63 therefore acts as a dual regulator that activates *FLC* directly under non-vernalization conditions but represses *FLC* indirectly during vernalization through inducing *COOLAIR* and *COLDAIR*. Furthermore, genome-wide occupancy profile analyses indicated that the binding of WRKY63 to vernalization-induced genes increases after vernalization. In addition, WRKY63 binding is associated with decreased levels of the repressive marker Histone H3 Lysine 27 trimethylation (H3K27me3). Collectively, our results indicate that WRKY63 is an important flowering regulator involved in vernalization-induced transcriptional regulation.

Introduction

The flowering time of Arabidopsis (*Arabidopsis thaliana*) is regulated by complex gene regulation networks associated with different regulation pathways, including photoperiod, autonomous and vernalization pathways (Hepworth and Dean, 2015). FLOWERING LOCUS T (FT) and SUPPRESSOR OF OVEREXPRESSION OF CO 1 (SOC1) are two key integrators perceiving these pathways. In the autonomous and vernalization pathways, the MADS-box transcription factor FLOWERING LOCUS C (FLC) acts as a repressor of *FT* and *SOC1* (Michaels and Amasino, 2001; Hepworth et al., 2002; Searle et al., 2006). The repression of *FLC* is mediated by the conserved chromatin-modifying complex Polycomb Repression Complex 2 (PRC2) (Gendall et al., 2001; De Lucia et al., 2008; Kim and Sung, 2013). Prolonged exposure to cold triggers the increased enrichment of PRC2 and increased levels of the repressive histone mark Histone H3 Lysine 27 trimethylation (H3K27me3) at *FLC* chromatin

Received March 08, 2022. Accepted May 21, 2022. Advance access publication June 16, 2022

(De Lucia et al., 2008; Kim and Sung, 2013). Two *Arabidopsis* long noncoding RNAs (lncRNAs), *COLD INDUCED LONG ANTISENSE INTRAGENIC RNA* (*COOLAIR*) and *COLD ASSISTED INTRONIC NONCODING RNA* (*COLDAIR*), are originated from the 3′ end and the first intron of *FLC*, respectively. The expression of both *COOLAIR* and *COLDAIR* is induced by vernalization. Furthermore, *COOLAIR* and *COLDAIR* repress *FLC* transcription by increasing the H3K27me3 level via interacting with the PRC2 complex (Swiezewski et al., 2009; Heo and Sung, 2011; Marquardt et al., 2014; Kim et al., 2017). In addition, *COOLAIR* and *COLDAIR* are also associated with DNA folding and the loop structure of *FLC* to repress *FLC* expression (Sun et al., 2013; Kim et al., 2017). These findings demonstrate the importance of *COOLAIR* and *COLDAIR* in *FLC* expression. However, the molecular mechanism of how *COOLAIR* and *COLDAIR* are transcriptionally regulated remains elusive.

The WRKY protein family is one of the largest groups of transcription factors in plants (Llorca et al., 2014). All WRKY transcription factors contain zinc-finger-like motifs and one or two WRKY domains (Eulgem et al., 2000). The WRKY domain is a DNA-binding region of approximately 60 amino acids composed of the conserved amino acid sequence WRKYGQK (Rushton et al., 1995). The WRKY transcription factors containing two WRKY domains are classified as group I, whereas most WRKY transcription factors containing one WRKY domain are categorized as group II (Eulgem et al., 2000). Both of these groups have the C2H2-type zinc-finger motif (Eulgem et al., 2000). There is a small group of WRKY transcription factors containing the C2HC-type zinc-finger motif with one WRKY domain that are classified as group III (Eulgem et al., 2000). Four members of *Arabidopsis* group-IIIa WRKY transcription factors, namely WRKY63, WRKY64, WRKY66 and WRKY67, share two highly conserved domains on the N-terminus and the WRKY domain on the C-terminus (Kalde et al., 2003). The biological function of these group-IIIa WRKY transcription factors remains largely unknown. Although members of the WRKY protein family are involved in biotic/abiotic stress responses, vegetative growth, and reproductive development, only a few of them have been reported to regulate flowering time (Li et al., 2016b; Yu et al., 2016; Zhang et al., 2018). Members of the group-IIc WRKY transcription factors in *Arabidopsis*, including WRKY12, WRKY13, WRKY71 and WRKY75, are involved in flowering (Li et al., 2016b; Yu et al., 2016; Zhang et al., 2018). WRKY71 promotes flowering by directly activating *FT* and *LEAFY* (*LFY*), accelerating transition from shoot apical meristems to floral meristems (Yu et al., 2016). WRKY12, WRKY13, and WRKY75 are involved in GA signaling and modulate flowering time through interacting with DELLA proteins (Li et al., 2016b; Zhang et al., 2018). In addition, the group-I WRKY34 can repress *FLC* indirectly by activating ubiquitin-E3 ligase *CULLIN3A* (*CUL3A*) to enhance degradation of the *FLC* activator FRIGIDA (FRI) (Hu et al., 2014).

Arabidopsis WRKY63, also named as ABA OVERLY SENSITIVE 3 (ABO3), is a member of group-IIIa WRKY transcription factors. Previous studies have demonstrated that WRKY63 plays a role in ABA response and drought tolerance by activating *ABSCISIC ACID RESPONSIVE ELEMENTS-BINDING FACTOR 2* (*ABF2*) (Ren et al., 2010). In addition, WRKY63 can also regulate stress responses of mitochondrial target proteins by activating *ALTERNATIVE OXIDASE 1a* (*AOX1a*) (Van Aken et al., 2013). In this study, we found that WRKY63 functions as a transcriptional activator of *FLC*. Furthermore, WRKY63 is involved in vernalization-induced flowering regulation by activating the expression of the lncRNAs *COOLAIR* and *COLDAIR*.

Results

WRKY63 is a transcriptional activator involved in flowering time regulation

Previous studies indicated that WRKY63 is involved in ABA and stress responses by regulating *ABF2* and *AOX1a* (Ren et al., 2010; Kim et al., 2017). To further investigate the biological function of WRKY63, the two *wrky63* mutant lines *wrky63-1* and *wrky63-2* (*abo3*) were obtained from *The Arabidopsis Information Resource* (TAIR; www.arabidopsis.org). *wrky63-1* and *wrky63-2* have T-DNA inserted in the promoter and third exon of the *WRKY63* locus, respectively (Supplemental Figure S1, A and B). Homozygous *wrky63-1* and *wrky63-2* lines were identified by reverse transcription quantitative PCR (RT-qPCR) analysis. Although the *WRKY63* transcript was detected in both *wrky63-1* and wild-type (WT), the expression of *WRKY63* was decreased in *wrky63-1*, indicating that it is a *WRKY63* knock-down line (Supplemental Figure S1, C and D). By contrast, the *WRKY63* transcript was absent in *wrky63-2*, indicating that it is a *WRKY63* knockout line (Supplemental Figure S1, C and D). Both *wrky63-1* and *wrky63-2* displayed an early flowering phenotype in both long-day (LD, 16 h light and 8 h dark) and short-day (SD, 8 h light and 16 h dark) conditions (Supplemental Figure 1, A and E), suggesting that WRKY63 is involved in flowering time regulation.

WRKY63 has been identified to be a transcriptional activator by using transcriptional activity assays in yeast (Ren et al., 2010). To further confirm whether WRKY63 can act as a transcriptional activator in planta, we conducted transient transcriptional activity assays in *Arabidopsis* protoplasts. WRKY63 fussed with the GAL4 DNA binding domain at the N-terminus (GALBD-WRKY63) was analyzed for whether it can activate the *Firefly LUCIFERASE* reporter with the GAL4 binding sites (GAL4BS) in the promoter. The GAL4 DNA binding domain fused with the VP16 activation domain (GAL4BD-VP16) was used as a positive control (Figure 1B). We found that the *LUCIFERASE* reporter can be activated by GAL4BD-WRKY63 (Figure 1C), indicating that WRKY63 can act as a transcriptional activator in *Arabidopsis*.

WRKY63 is a transcriptional activator of *FLC*

To investigate the function of WRKY63 in flowering time regulation, we analyzed expression of the core floral regulator genes *FT*, *SOC1*, and *FLC* in *wrky63* mutants. The expression

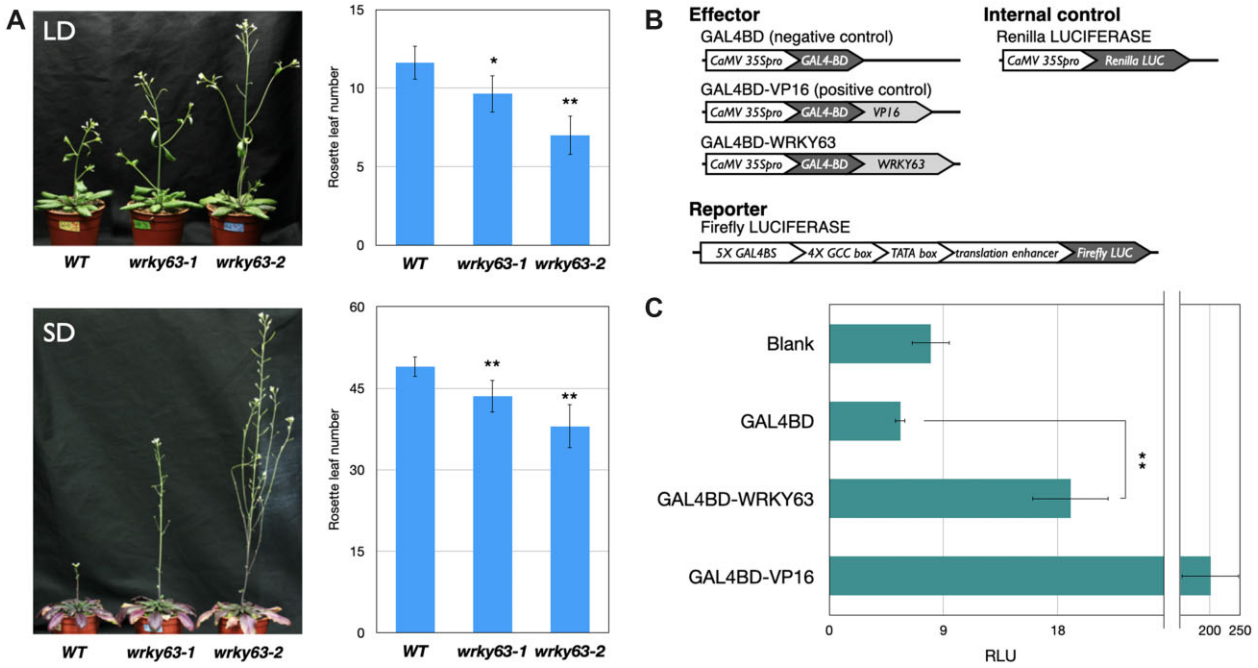

Figure 1 *Arabidopsis* WRKY63 is a transcriptional activator and is involved in flowering regulation. A, The flowering phenotypes and rosette leaf numbers of WT and *wrky63* mutants under LD and SD. $^{**}P < 0.001$, $^{*}P < 0.01$ (Student's *t* test). Values are means ±SD. The experiments were performed with three biological replicates showing comparable results. B, Schematic structure of the effectors, reporter, and internal control used in the transient transcriptional activity assays. C, Transient transcriptional activity assays of WRKY63. GAL4BD-WRKY63 activated the expression of *firefly LUCIFERASE* (*firefly LUC*). Blank: no effector was added. GAL4BD was used as a negative control. GAL4BD fused with the activation domain VP16 (GAL4BD-VP16) was used as a positive control. Values are means ±SD. $^{**}P < 0.001$ (Student's *t* test). The experiments were performed with three biological replicates showing comparable results. RLU, relative luciferase activity.

of *FT* and *SOC1* was significantly increased, but the expression of *FLC* was decreased in both *wrky63-1* and *wrky63-2* compared to WT (Figure 2A), suggesting that WRKY63 acts upstream of *FT*, *SOC1*, and *FLC* (Figure 2A). To analyze the genetic interaction of WRKY63 with *FT* and *FLC* in flowering time control, we generated the *wrky63/ft* and *wrky63/flc* double mutants. *wrky63/ft* showed a late flowering phenotype similar to *ft* (Supplemental Figure S2), suggesting that WRKY63 acts upstream of *FT* in flowering time control. Compared to WT, *wrky63/flc* showed an early flowering phenotype similar to *wrky63-2* and *flc* (Supplemental Figure S3).

To further investigate whether WRKY63 can directly activate *FLC* expression, we generated the *FLCpro::FLC-FLAG* construct containing the *FLC* coding sequence (CDS) fused with $3 \times FLAG$ driven by the *FLC* native promoter. *FLCpro::FLC-FLAG* was co-expressed with *35Spro::WRKY63-GFP* or *35Spro::mcherry* control in *Nicotiana benthamiana* leaves by using *Agrobacterium*-mediated infiltration. Compared to the negative control, the protein level of FLC-FLAG was increased when *FLCpro::FLC-FLAG* was co-expressed with *35Spro::WRKY63*, suggesting that WRKY63 can induce *FLC* expression (Figure 2B).

We also generated *WRKY63pro::WRKY63-GFP* transgenic lines, in which the *WRKY63* genome sequence containing its native promoter fused with the *GFP* epitope tag was transformed into *wrky63-2*. The early flowering phenotype of *wrky63-2* was rescued by expressing *WRKY63pro::WRKY63-GFP* (Supplemental Figure S4), suggesting that WRKY63-GFP is functional. The binding of WRKY63 to *FLC* was analyzed by chromatin immunoprecipitation followed by quantitative PCR (ChIP-qPCR). ChIP assays were performed with the anti-GFP antibody using *WRKY63pro::WRKY63-GFP* transgenic seedlings. We found that WRKY63 can be enriched in the *FLC* promoter and the transcription starting site regions, indicating that WRKY63 can activate *FLC* by directly targeting (Figure 2, C and D). Previous studies indicate that the expression of *FLC* is highly associated with H3K27me3 level changes (Gendall et al., 2001; De Lucia et al., 2008; Kim and Sung, 2013). We further investigated whether WRKY63 affects the level of H3K27me3 on the *FLC* locus. Compared to WT, we found that the H3K27me3 level of *FLC* was increased in *wrky63* (Figure 2E). Collectively, these results indicated that WRKY63 can directly target *FLC* and activate *FLC* expression. Furthermore, WRKY63-induced *FLC* expression is associated with decreased H3K27me3.

WRKY63 is involved in vernalization-induced flowering

Previous studies indicated that FLC is involved in vernalization-induced flowering (De Lucia et al., 2008; Swiezewski et al., 2009; Heo and Sung, 2011; Kim and Sung, 2013). To investigate whether WRKY63 is involved in vernalization-induced flowering, *wrky63* mutant plants were treated with 0, 2, and 4 weeks of vernalization. The flowering

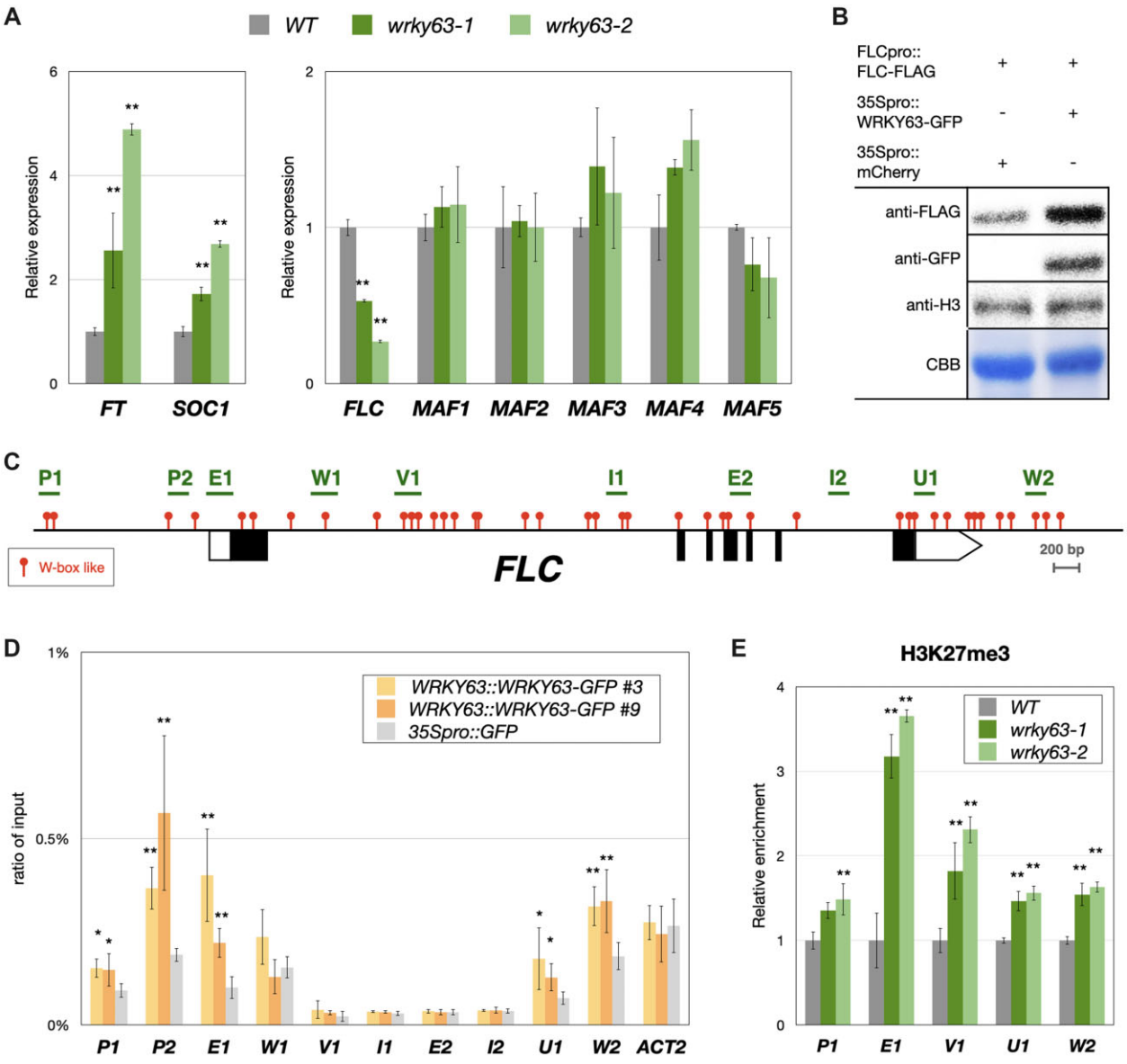

Figure 2 WRKY63 can activate *FLC* by direct targeting. A, The relative expression of *FT*, *SOC1*, *FLC*, *MAF1*, *MAF2*, *MAF3*, *MAF4*, and *MAF5* in *wrky63-1*, *wrky63-2*, and WT *Arabidopsis*. B, Western blot of FLCpro::FLC-FLAG in *Agrobacterium*-infiltrated *Nicotiana benthamiana* leaves transformed with 35Spro::WRKY-GFP or the 35Spro::mcherry control. Western blots were performed with indicated antibodies, H3 and total proteins stained with CBB were used as the loading control. CBB, coomassie brilliant blue. C, The schematic structure of the *FLC* genome. The red dots indicate W-boxes like motifs (TGAC), and the regions analyzed for ChIP-qPCR are marked with green lines. D, Binding of WRKY63-GFP to *FLC* identified by ChIP-qPCR assays. Fourteen-day-old *WRKY63pro::WRKY63-GFP* transgenic plants were used for ChIP assays using an anti-GFP antibody. The *35Spro::GFP* transgenic plants were used as a control. The amount of immunoprecipitated DNA was quantified by qPCR. Values represent the average immunoprecipitation efficiencies (%) against the total input DNA, and *ACT2* was used as a negative control. E, ChIP analysis of H3K27me3 levels on the *FLC* locus. Fourteen-day-old plants were used for ChIP assays. The amounts of DNA after ChIP were quantified by qPCR and normalized to *TA3*. The values of these qPCR assays are means ±SD. These experiments were performed with three biological replicates showing comparable results. $^{**}P < 0.001$, $^{*}P < 0.01$ (Student's *t* test).

time of WT plants was decreased after vernalization. However, the flowering time of *wrky63* mutants was not reduced after the vernalization treatment (Figure 3A; Supplemental Figure S5), indicating that *wrky63* mutants are insensitive to vernalization.

We further analyzed whether the expression of *WRK63* is affected by vernalization. *WRKY63pro::WRKY63:GFP* transgenic seedlings were analyzed using a fluorescent microscope. We found that the GFP signal was presented in the leaves and root-tips of the transgenic plants (Figure 3B; Supplemental Figure S6). Interestingly, the fluorescence intensity of GFP was increased after vernalization treatment (Figure 3, B–D; Supplemental Figure S6). Western-blot analysis indicated that the protein level of WRKY63 was increased after vernalization (Figure 3E). In addition, the transcript of *WRKY63* was also increased after vernalization (Figure 3F). These results indicated

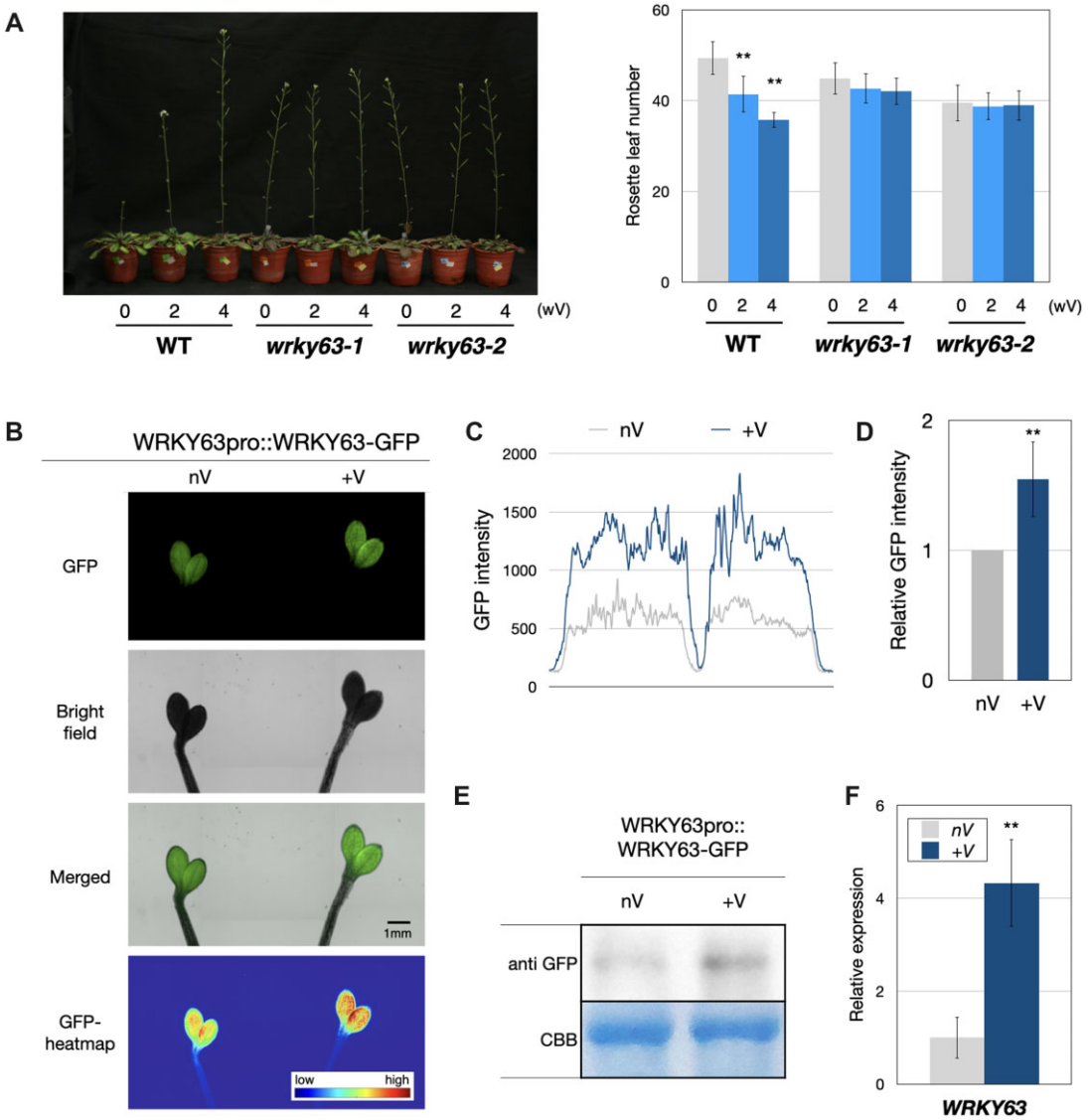

Figure 3 WRKY63 is induced by vernalization and is involved in vernalization-induced flowering. A, The flowering phenotypes and rosette leaf numbers of WT and *wrky63* mutants under 0, 2, and 4 weeks of vernalization treatments in SD. At least 20 plants of each line were counted for the rosette leaf numbers at flowering. Values are means ±SD. **: $P < 0.001$ (Student's *t* test). The experiments were repeated 3 times with comparable results. wV, weeks of vernalization. B, GFP fluorescence signal in *WRKY63pro::WRKY63:GFP* transgenic plants without vernalization (nV) or with 4 weeks of vernalization (+V). The experiments were performed with three biological replicates showing comparable results. Bar = 1 mm. C and D, Quantification of GFP fluorescent intensity (C) and the relative GFP fluorescent intensity (D) in *WRKY63pro::WRKY63:GFP* transgenic plants without vernalization (nV) or with 4 weeks of vernalization (+V). The *X*-axis represents the detected section of cotyledons, *Y*-axis fluorescence indicates the value of GFP intensity. Values of relative GFP intensity are normalized means ±SD. **$P < 0.001$. At least 10 leaves for each treatment were counted for the GFP intensity. E, Western blot of WRKY63pro::WRKY63:GFP in transgenic plants without vernalization (nV) or with 4 weeks of vernalization (+V). The western blots were performed with the indicated antibody, and the total protein stained with CBB was used as the loading control. F, The relative expression of *WRKY63* in WT *Arabidopsis* without vernalization (nV) or with 4 weeks of vernalization (+V). **$P < 0.001$ (Student's *t* test). Values are means ±SD. The experiments were performed with three biological replicates showing comparable results. CBB, coomassie brilliant blue.

that the expression of *WRKY63* can be induced by vernalization. Collectively, our results suggested that WRKY63 is involved in vernalization-induced flowering.

WRKY63 is a transcriptional activator of the lncRNAs *COOLAIR* and *COLDAIR*

To further investigate how WRKY63 is involved in vernalization-induced flowering, we analyzed the expression of *FLC* after the vernalization treatment. After vernalization, *FLC* expression was decreased in WT but not in the *wrky63* mutants (Figure 4, A and B), suggesting that vernalization-repressed expression of *FLC* is dependent on WRKY63. The *Arabidopsis* lncRNAs *COOLAIR* and *COLDAIR* can be induced by vernalization, and both of them can repress the expression of *FLC* (Swiezewski et al., 2009; Heo and Sung, 2011; Marquardt et al., 2014; Kim et al., 2017). Interestingly,

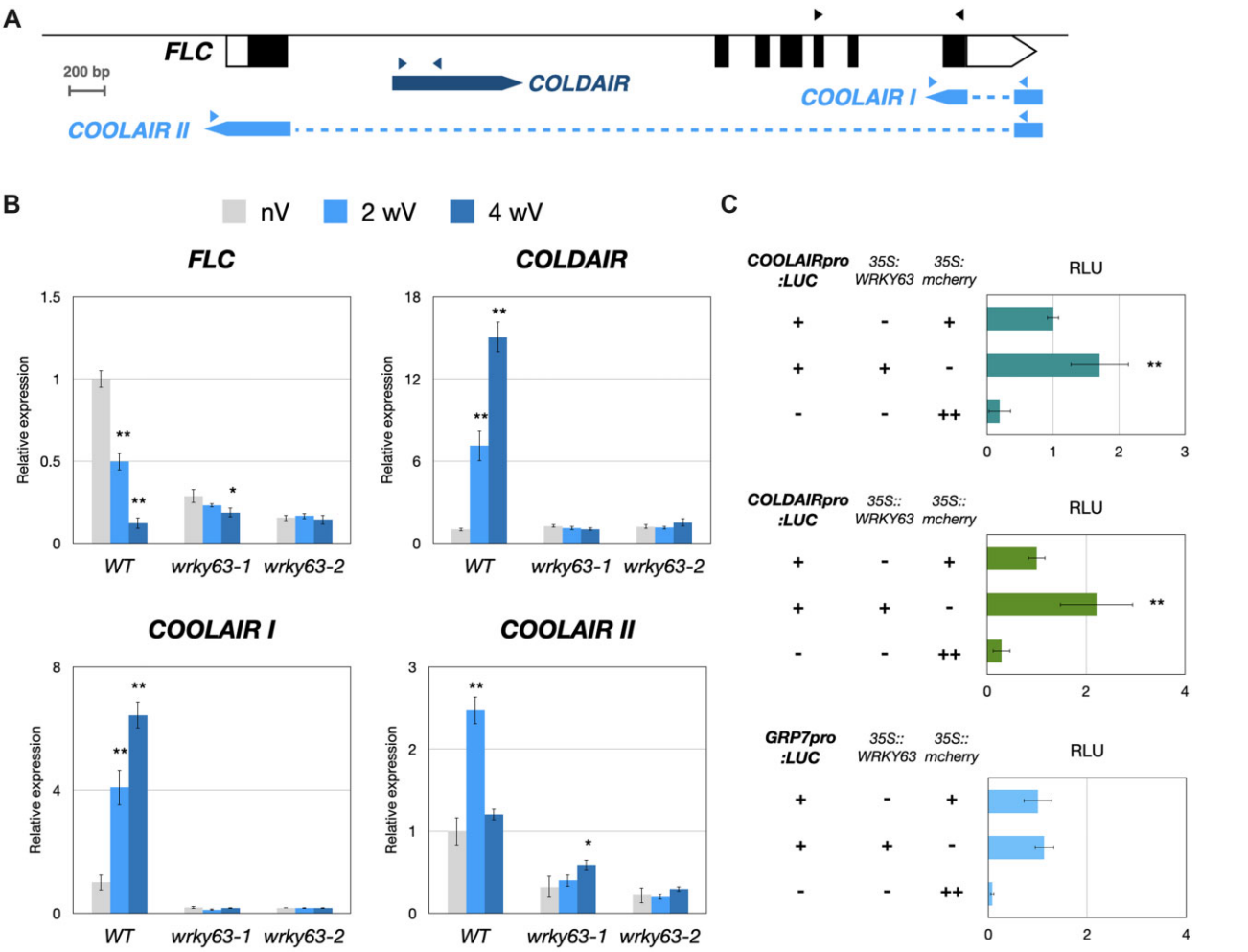

Figure 4 The expression of *COOLAIR* and *COLDAIR* is activated by WRKY63. A, The *FLC* structure and the fragments used for the RT-qPCR assay. Arrows indicate the primer sets in RT-qPCR. The blocks represent transcribed regions of *FLC*, *COLDAIR* and *COOLAIR*. The dashed lines indicate intron regions. B, The relative expression of *FLC*, *COLDAIR*, Class I *COOLAIR* (*COOLAIR I*), and Class II *COOLAIR* (*COOLAIR II*) in *wrky63-1*, *wrky63-2*, and WT treated with 0, 2, or 4 weeks of vernalization (nV, 2wV, and 4wV). C, Transient transcriptional activity assays of *COOLAIRpro::LUC*, *COLDAIRpro::LUC*, and *GRP7pro::LUC*. The *firefly LUCIFERASE* (*LUC*) driven by the *COOLAIR* promoter, *COLDAIR* promoter, or *GRP7* promoter were co-transformed with the effector *35S::WRKY63* and the *35Spro::mcherry* control. RLU represents firefly LUCIFERASE normalized by co-expressed *35Spro::Renilla luciferase*. The value of above assays represents means ±SD. These experiments were performed with three biological replicates showing comparable results. $^{**}P < 0.001$, $^{*}P < 0.05$ (Student's *t* test). RLU, relative light units.

we found that the expression of *COOLAIR* and *COLDAIR* was strongly increased in WT after vernalization treatment, but not in the *wrky63* mutants (Figure 4, A and B). These results suggested that vernalization-induced *COOLAIR*/*COLDAIR* expression is dependent on WRKY63. To further confirm whether WRKY63 can activate *COOLAIR*/*COLDAIR* expression, *COOLAIR*/*COLDAIR* promoter-driven *LUCIFERASE* constructs (*COOLAIRpro::LUC*/*COLDAIRpro::LUC*) were co-expressed with *35Spro::WRKY63* or the *35Spro::mcherry* control. We found that the expression of *COOLAIRpro::LUC* and *COLDAIRpro::LUC* was significantly increased when co-expressed with *WRKY63*, but not with the *35Spro::mcherry* control (Figure 4C). By contrast, the *GLYCINE RICH PROTEIN 7* (*GRP7*) promoter-driven *LUCIFERASE* construct (*GRP7pro::LUC*), which was used as a control, did not show increased expression when co-expressed with *WRKY63* (Figure 4C). Together, these data indicated that WRKY63 is a transcriptional activator of *COOLAIR* and *COLDAIR*.

We further tested the *wrky63* mutant for its vernalization response by the introgression of *wrky63* into the FRIcol (Col-0 with a functional *FRI* allele) genetic background (Gazzani et al., 2003). We found that *FRI*/*wrky63* was also insensitive to vernalization (Supplemental Figure S7, A and B). The gene expression pattern was also analyzed in *FRIcol* and *FRI*/*wrky63*. We found that the expression of *FLC* was significantly decreased in *FRI*/*wrky63* compared to *FRIcol* (Supplemental Figure S7C). In addition, we also found that the expression of *COOLAIR* was decreased in *FRI*/*wrky63* compared to *FRIcol* (Supplemental Figure S7C). These results indicated that vernalization-induced *COOLAIR* expression is dependent on WRKY63.

The binding of WRKY63 to *FLC* under vernalization (V) or non-vernalization (nV) treatment was further analyzed by ChIP-qPCR using *WRKY63pro::WRKY63:GFP* transgenic seedlings. We found that the binding of WRKY63 on the first intron (W1 and V1) and down-stream regions (U1 and W2) of *FLC* was significantly increased after vernalization treatment (Figure 5, A and B). Interestingly, two WRKY63 binding sites, W2 and W1, are located in the 5′ upstream regions of the transcription start sites (TSS) of *COOLAIR* and *COLDAIR*, respectively (Figure 5A). Collectively, these results suggested that WRKY63 can directly target the *FLC* locus to activate *FLC* under non-vernalization conditions. Furthermore, vernalization increases the binding of WRKY63 to the *COOLAIR/COLDAIR* promoter, which activates *COOLAIR/COLDAIR* transcription and suppresses the expression of *FLC*.

Previous studies have revealed that the vernalization-repressed expression of *FLC* is associated with PRC2-mediated H3K27me3 enrichment (De Lucia et al., 2008; Swiezewski et al., 2009; Heo and Sung, 2011; Kim and Sung, 2013). To further investigate whether WRKY63 is involved in the regulation of histone modifications, we also analyzed the H3K27me3 and H3 acetylation (H3Ac) levels in *wrky63* treated with vernalization (+V) or non-vernalization (nV). The H3K27me3 level of *FLC* in *wrky63* was increased compared to WT before vernalization (Figure 5C). Furthermore, the H3K27me3 level of *FLC* was significantly increased after vernalization in WT. By contrast, the H3K27me3 level of *FLC* in *wrky63* was not changed after vernalization (Figure 5C). In addition, the H3Ac level of *FLC* was not substantially affected by vernalization in both *wrky63* and WT (Supplemental Figure S8). These results indicated that WRKY63-induced gene expression is associated with decreased H3K27me3 levels.

Genome-wide occupancy profiles of WRKY63

To investigate the genome-wide function of WRKY63 in gene regulation, we mapped the genome-wide occupancy of WRKY63. Chromatin immunoprecipitation followed by sequencing (ChIP-seq) was carried out to identify the WRKY63-targeted genomic regions using *WRKY63pro::WRKY63:GFP* transgenic plants under vernalization or non-vernalization treatment. Similar to the ChIP-qPCR data, the genome browser views of WRKY63 ChIP-Seq data also show that WRKY63 can target the *FLC* promoter and first exon, and vernalization increased the binding of WRKY63 on the first intron and downstream regions (Figure 6A). Compared to the *Arabidopsis* genomic region distribution, we found that the enrichment of WRKY63 was higher in the 1-kb promoter regions, but lower in the exon regions (Figure 6B). The genomic distribution ratio of WRKY63 was similar among vernalization and non-vernalization treatments (Figure 6B). In addition, we identified many cis-elements that were enriched

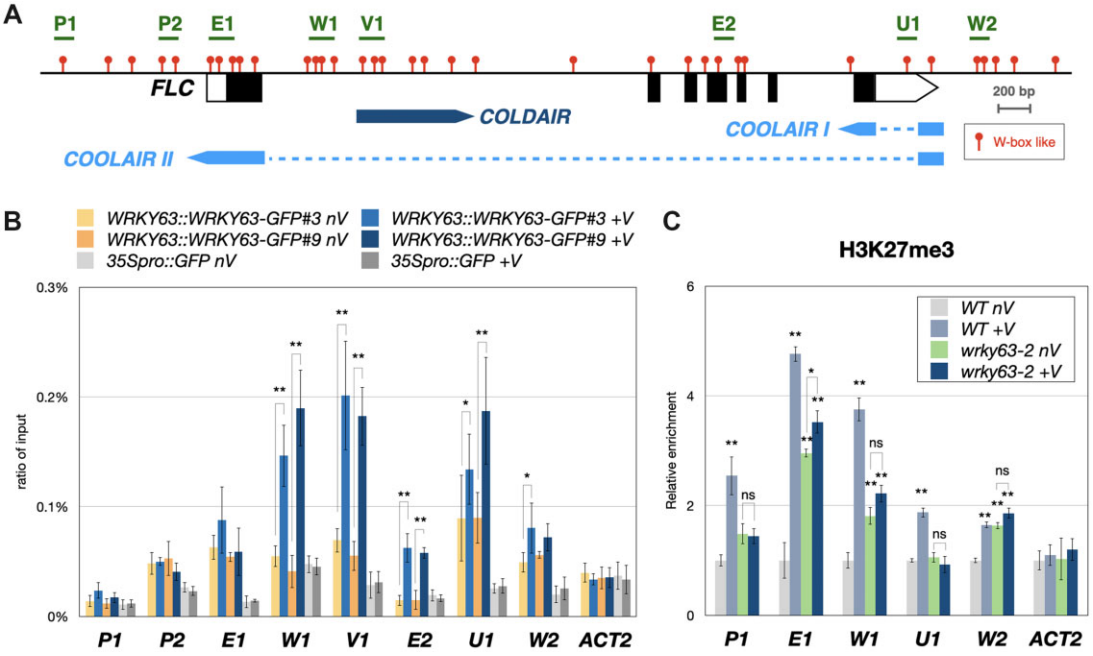

Figure 5 Binding of WRKY63 and the H3K27me3 level on the *FLC* locus in vivo. A, The schematic structure of the *FLC* genome. The blocks represent transcribed regions of *FLC*, *COLDAIR* and *COOLAIR*. The dashed lines indicate intron regions. B, Binding of WRKY63pro::WRKY63:GFP to *FLC* identified by ChIP-qPCR assays. Fourteen-day-old *WRKY63pro::WRKY63:GFP* transgenic plants without vernalization (nV) or with 4 weeks of vernalization (+V) were used for ChIP assays using an anti-GFP antibody. The *35Spro::GFP* transgenic plants were used as a control. The amount of immunoprecipitated DNA was quantified by qPCR. Values represent the average immunoprecipitation efficiencies (%) against the total input DNA, and *ACT2* was used as a negative control. C, ChIP analysis of H3K27me3 levels on the *FLC* locus. Plants without vernalization (nV) or with 4 weeks of vernalization (+V) were used for ChIP assays. The amounts of DNA after ChIP were quantified by qPCR and normalized to *TA3*. Error bars indicate SD from three biological replicates. $^{*}P < 0.01$, $^{**}P < 0.001$, ns: no significant difference (Student's *t* test).

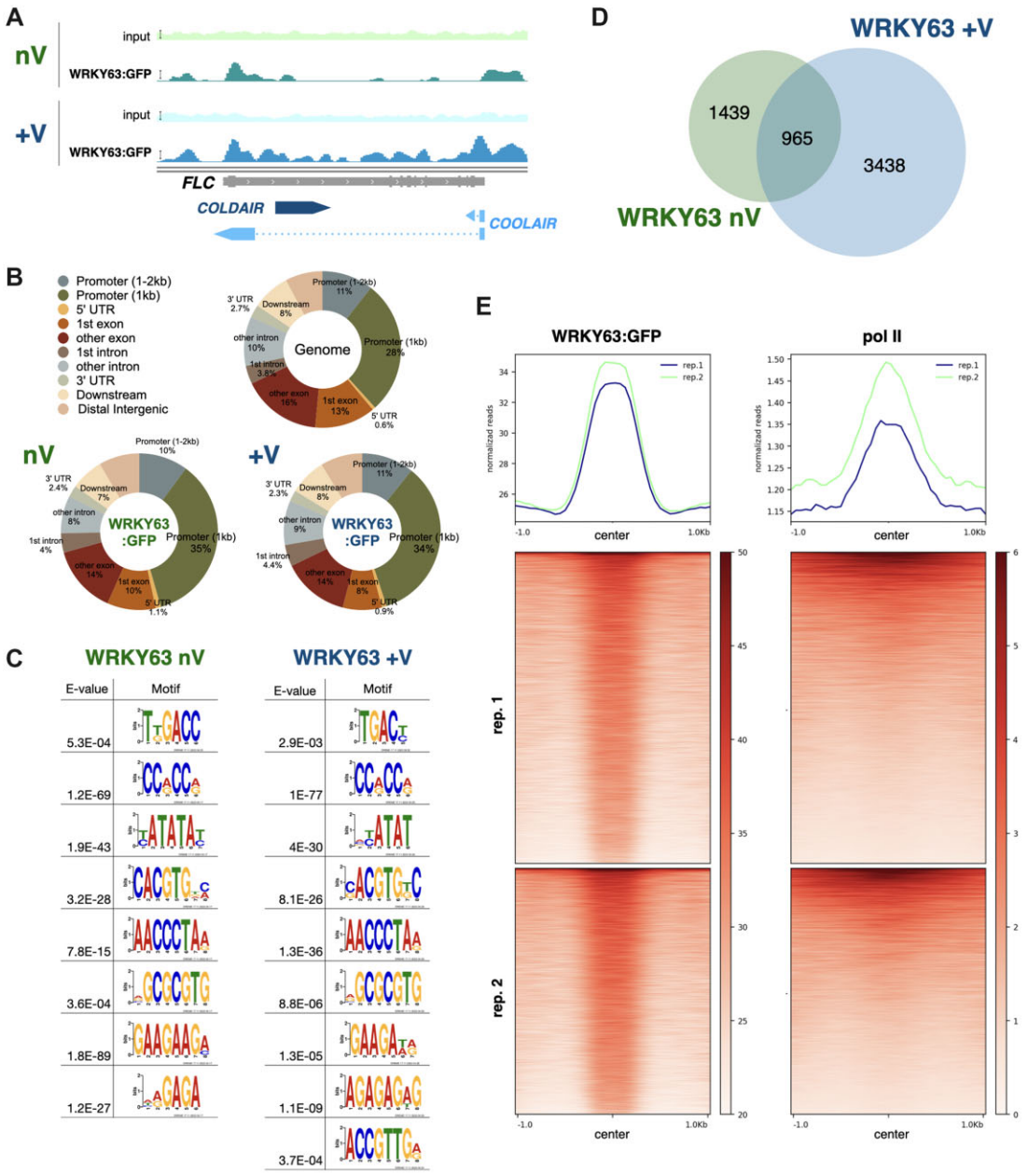

Figure 6 Genome-wide occupancy profiles of WRKY63. A, IGV showing the binding of WRKY63 on the *FLC* locus without (nV) or with (+ V) vernalization. Bars: normalized reads = 25. B, Pie charts showing the distribution of WRKY63 annotated genic and intergenic regions in the genome. C, The DNA binding motifs significantly enriched in the WRKY63 binding sites. D, A Venn diagram showing the overlap between WRKY63 targeted genes among vernalization (WRKY63 + V) and non-vernalization (WRKY63 nV) treatments. E, Heat map representation of the occupancy of WRKY63 and RNA polymerase II (pol II) in the WRKY63 occupied genomic region. Each horizontal line represents a WRKY63 binding region, and the signal intensity is shown for the occupancy of WRKY63 and pol II (center). Columns show the genomic region surrounding each WRKY63 peak. Signal intensity is indicated by the shade of heatmap.

within the WRKY63 binding sites, including TGACC/T, CCRCCR, TATA-box, G-box (CACGTG), AACCCTA and AG/AAG sequences (Figure 6C). The enriched cis-element TGACC/T is the W-box like motif, which is found to be targeted by many WRKY family transcription factors (Eulgem et al., 2000; Maeo et al., 2001). We found that the WRKY63 enriched cis-elements of vernalization and non-vernalization treatments were similar (Figure 6C). Taken together, these results suggested that the genomic distribution ratio and the DNA binding motifs of WRKY63 are not affected by vernalization.

However, we also found that the number of WRKY63-targeted genes is increased after vernalization (Figure 6D). Many of the WRKY63-targeted genes under vernalization were not targeted by WRKY63 without vernalization (Figure 6D), suggesting that WRKY63 binds to a subset of

genes only after vernalization. These results indicated that WRKY63 might be involved in the vernalization-induced gene activation. We further classified the WRKY63 target genes into three different groups, namely the genes specific for vernalization, those specific for non-vernalization, and those for both vernalization and non-vernalization. These WRKY63-targeted genes were further analyzed according to Gene Ontology Biological Processes (GO-BP). We found that the WRKY63 target genes are involved in different types of hormone responses, stress responses, and development pathways (Supplemental Figure S9). Interestingly, we found that the GO term "vernalization response (GO:0010048)" was only enriched in the genes specifically targeted by WRKY63 after vernalization (Supplemental Figure S9). By contrast, the genes specifically targeted under non-vernalization were more associated with the light response and circadian rhythm, but less associated with developmental responses (Supplemental Figure S9). These results suggested that WRKY63 may be involved in different regulation processes under vernalization and non-vernalization.

We also compared the WRKY63-occupied genomic regions with the previously published ChIP-Seq data of RNA polymerase II (pol II) (Liu et al., 2018). The plotprofile and plot heatmap analyses indicate that the center of WRKY63-binding regions was highly associated with the enrichment of pol II (Figure 6E). These results support that WRKY63 can act as a transcriptional activator and may be associated with the regulation of transcription initiation.

WRKY63 is associated with vernalization-induced gene activation and decreased H3K27me3

We further investigated the function of WRKY63 in the vernalization-induced gene activation. A subset of vernalization-induced genes was previously identified by the RNA-sequencing data of *Arabidopsis* treated with vernalization (Gibbs et al., 2018). We found that the binding of WRKY63 was highly enriched near the TSS of these vernalization-induced genes. In addition, the binding of WRKY63 on these genes was substantially increased after vernalization (Figure 7A). We also identified a subset of genes with decreased H3K27me3 levels after vernalization from the published ChIP-seq datasets (Xi et al., 2020). Similarly, the binding of WRKY63 to these genes with decreased H3K27me3 was substantially increased after vernalization (Figure 7B). Compared to the non-vernalization-specific targets of WRKY63, the vernalization-specific targets of WRKY63 tend to have high degrees of overlap with the vernalization-induced genes and the H3K27me3 decreased genes (Supplemental Figure S10).

To further analyze the function of WRKY63 in association with H3K27me3, we compared the H3K27me3 level in the WRKY63 targeted genomic regions under vernalization (WRKY63 + V) or non-vernalization (WRKY63 nV) treatments. Interestingly, we found that the H3K27me3 level on the targeted regions of WRKY63 + V was substantially decreased after vernalization (Figure 7C). By contrast, the H3K27me3 level on the binding regions of WRKY63-nV was not changed (Figure 7C). Furthermore, the relative H3K27me3 levels of the vernalization-specific target genes of WRKY63 were substantially decreased after vernalization (Figure 7, D and E). Collectively, these results indicated that WRKY63 is involved in both gene activation and H3K27me3 decreasing induced by vernalization. However, a subset of vernalization-specific WRKY63 targets did not show decreased H3K27me3 after vernalization (Supplemental Figure S10), suggesting that in addition to H3K27 demethylation, other histone modifications may also be involved in WRKY63-regulated genes.

We selected several vernalization-induced genes that are targeted by WRKY63 with decreased H3K27me3 after vernalization for further analysis. Genome browser views of the RNA-seq data also indicated that the expression of these genes was increased after vernalization (Figure 8A). Furthermore, these vernalization-induced genes were also directly targeted by WRKY63, and the binding of WRKY63 was increased after vernalization (Figure 8A). We found that the expression of several cold-response genes was also decreased in *wrky63* compared to WT after vernalization, such as *C-REPEAT/DRE BINDING FACTOR 1* (*CBF1*) (Stockinger et al., 1997), *COLD-REGULATED 47* (*COR47*) (Guo et al., 1992), *KIN1* (Knight et al., 1996), *ACYL-LIPID DESATURASE2* (*ADS2*) (Chen and Thelen, 2013), and *CA2 + -BINDING PROTEIN 1* (*AtCP1*) (Knight et al., 1996; Delk et al., 2005) (Figure 8B). Recent studies indicate that the HD2-type histone deacetylase HD2C and the flowering regulator GIGANTEA (GI) are involved in cold responses (Fornara et al., 2015; Park et al., 2018; Lim et al., 2020). We found that vernalization-induced expression of *HD2C* and *GI* was decreased in *wrky63* (Figure 8B). Together, these results indicated that WRKY63 is required for the activation of vernalization-induced genes. In addition, the increased expression of these vernalization-induced genes was associated with decreased H3K27me3 after vernalization (Figure 8A). We further analyzed the H3K27me3 levels of these genes in *wrky63* using ChIP-qPCR. Vernalization reduced H3K27me3 levels in WT (Figure 8C). However, the H3K27me3 levels of these genes in *wrky63* were significantly higher compared to WT after vernalization (Figure 8C). Collectively, these results indicated that WRKY63 is associated with the decreased H3K27me3 of the vernalization-induced genes.

Discussion

Arabidopsis WRKY63 is a member of group-IIIa WRKY transcription factors (Eulgem et al., 2000). Previous studies have demonstrated that WRKY63 plays a role in ABA response and drought tolerance by directly targeting to the W-boxes of *ABF2* and *AOX1a* (Ren et al., 2010; Van Aken et al., 2013). In this study, we identified that WRKY63 functions as a transcriptional activator of *FLC* and is involved in the vernalization-induced flowering. The transcript and protein of WRKY63 are increased after vernalization. Furthermore, a subset of vernalization-induced genes can be activated by WRKY63. In addition to flowering, WRKY63-regulated genes

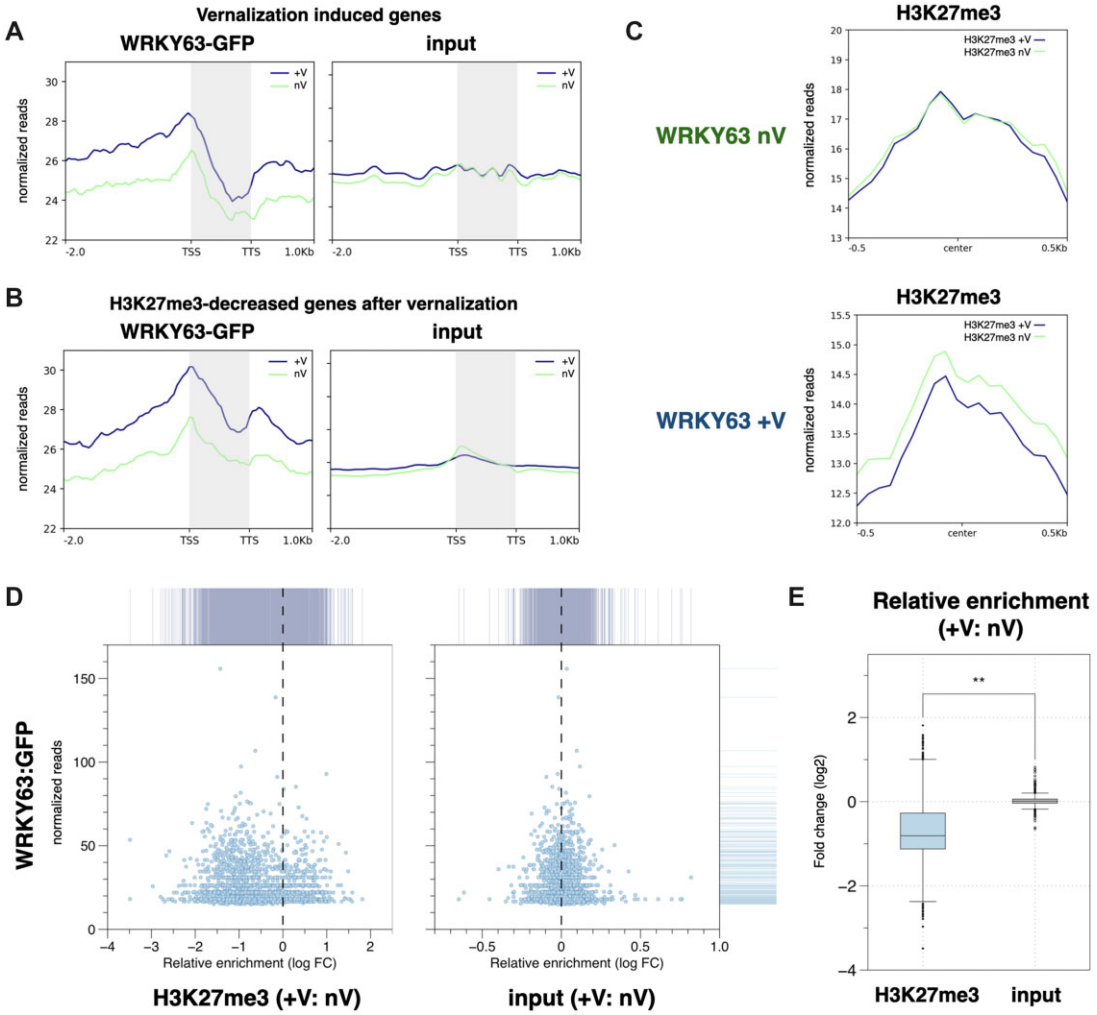

Figure 7 WRKY63 is associated with vernalization-induced gene activation and H3K27me3 demethylation. A and B, Metagene ChIP-seq binding profiles of WRKY63 among the vernalization-induced genes (A) and the H3K27me3-decreased genes after vernalization (B). The profile is from 2-kb upstream of the TSS to 1-kb downstream of the TTS, and the gene lengths were scaled to the same size. C, The mean density of H3K27me3 enrichment in the WRKY63 occupied regions under non-vernalization (WRKY63 nV) or vernalization (WRKY63 + V) treatments. The average H3K27me3 signal under vernalization (H3K27me3 + V) or non-vernalization (H3K27me3 nV) within 0.5-kb genomic regions flanking the center of WRKY63 peaks is shown. D, *X*–*Y* scatter plots showing the relative enrichment of H3K27me3 levels (+ V: nV) and the binding level of WRKY63 under vernalization with the vernalization-specific WRKY63 targeted genes. E, Boxplot showing the relative H3K27me3 level (+ V: nV) of the vernalization-specific WRKY63 targeted genes. Center line: median value; box limits: central 50% of the data, upper/lower quartiles: first/last 25% of the data; points: value of the outliers. $^{**}P < 0.001$ (Student's *t* test).

are also involved in the other development processes as well as hormone and stress responses. Recently, the genomic binding patterns of WRKY18, WRKY33, and WRKY40 were also investigated by using ChIP-seq (Birkenbihl et al., 2017). It was found that WRKY18 and WRKY40 are redundantly involved in flg22-induced defense responses (Birkenbihl et al., 2017). Our ChIP-seq analyses indicate that the enrichment of WRKY63 was higher in the promoter regions, but lower in the exon regions. In addition, the binding of WRKY63 is highly enriched in regions near the TSS. Similar binding patterns were also observed for WRKY18, WRKY33, and WRKY40 (Birkenbihl et al., 2017).

lncRNAs are involved in diverse gene regulation processes, including chromatin remodeling, histone modification, alternative splicing, and transcriptional activation (Wang et al., 2011; Bardou et al., 2014; Liu et al., 2015; Hung et al., 2020a). In *Arabidopsis*, the lncRNAs *COOLAIR* and *COLDAIR* are necessary for vernalization-induced *FLC* repression by increasing the occupancy of PRC2 at *FLC* chromatin (Swiezewski et al., 2009; Heo and Sung, 2011; Marquardt et al., 2014; Kim et al., 2017). The expression of *COOLAIR* and *COLDAIR* is highly increased under prolonged cold treatment (Swiezewski et al., 2009; Heo and Sung, 2011; Marquardt et al., 2014; Kim et al., 2017). However, the molecular mechanism of how *COOLAIR* and *COLDAIR* are transcriptionally activated remains elusive. In this study, we found that WRKY63 can directly bind to the *FLC* locus. Furthermore, WRKY63 binding on the promoters of

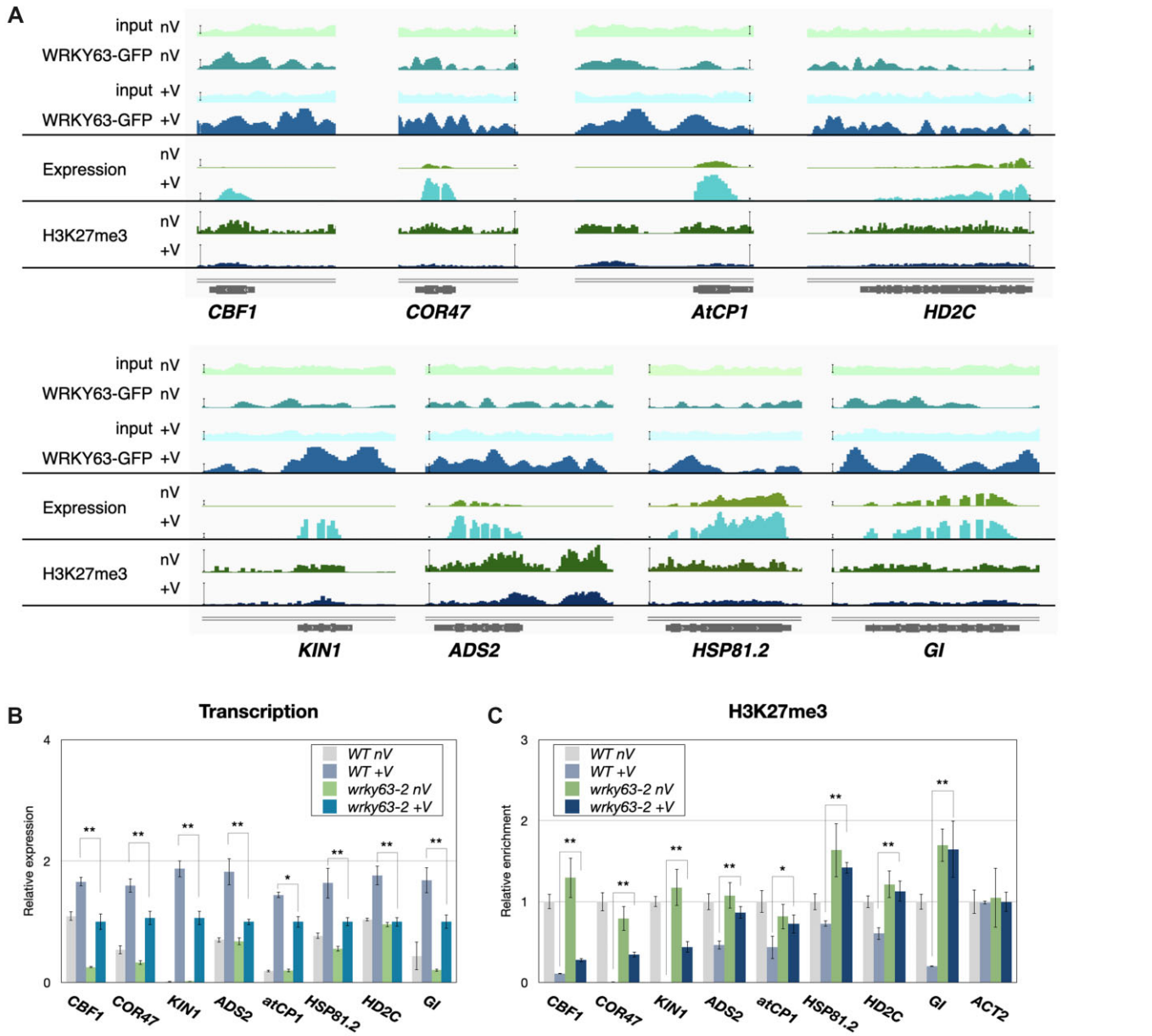

Figure 8 The WRKY63 binding, expression and H3K27me3 level of WRKY63 regulated genes. A, IGV showing the WRKY63 binding, expression, and H3K27me3 level of selected genes. Bars: normalized reads = 25. B and C, Expression (B) and H3K27me3 patterns (C) in WT and *wrky63* mutants. Expression of the indicated genes was analyzed by RT-qPCR. *UBQ10* was used as an internal control. ChIP assays were performed with the H3K27me3 antibody. The amounts of DNA after ChIP were quantified by qPCR and normalized to *TA3*. Error bars correspond to standard derivations. $^{*}P < 0.05$; $^{**}P < 0.005$ (Student's *t* test). At least three independent biological replicates were performed with similar results.

COOLAIR and *COLDAIR* is significantly increased after vernalization. We also found that the vernalization-induced expression of *COOLAIR* and *COLDAIR* is decreased in the *wrky63* mutant compared to WT. In addition, WRKY63 can also activate the *LUC* reporter gene driven by *COOLAIR* and *COLDAIR* promoters in the transactivation assays. These results indicated that WRKY63 can act as a transcriptional activator of *COOLAIR* and *COLDAIR*. Our recent study has revealed that the expression of lncRNAs is associated with H3Ac/H3K4me2 changes regulated by the HDA6-LDL1/2 histone modification complex in *Arabidopsis* (Hung et al., 2020a). In addition, *COOLAIR* interacts with the FRI super-complex and was predicted to be involved in forming a loop on the *FLC* transcript during vernalization (Sun et al., 2013). It remains to be determined whether *COOLAIR* and *COLDAIR* activation mediated by WRKY63 is related to these processes. Intriguingly, we found that WRKY63 can target different genomic regions of the *FLC* locus. Although WRKY63 can bind to the *FLC* promoter and first exon without vernalization, the binding of WRKY63 on *COOLAIR* and *COLDAIR* promoters is increased after vernalization. These results suggested that WRKY63 can activate *FLC* under non-vernalization conditions and also activate *COOLAIR*/*COLDAIR* transcription to suppress the expression of *FLC*

during vernalization. However, the mechanism underlying the binding of WRKY63 to different regions of the *FLC* locus is still unclear. It is possible that WRKY63 may associate with different protein complexes under vernalization and non-vernalization conditions. It has been reported that the protein components of the PRC2 complex are different and can target different regions of *FLC* under vernalization and non-vernalization conditions (Wood et al., 2006; Swiezewski et al., 2009; Heo and Sung, 2011; Marquardt et al., 2014; Kim et al., 2017). Changed binding of WRKY transcription factors under specific stress conditions has also been reported (Rushton et al., 2010; Llorca et al., 2014; Li et al., 2016b). Genome-wide analyses of WRKY63 occupancy indicated that WRKY63-targeted genes are substantially changed after vernalization, suggesting that WRKY63 may regulate gene expression under different environmental conditions by targeting different genomic regions.

There are 21 JmjC domain-containing proteins in *Arabidopsis*, which can act as demethylases to remove methyl-group on lysine residues of histone proteins and are involved in developmental processes (Lu et al., 2008; Luo et al., 2014; Hung et al., 2020b, 2021). The KDM4 group of JmjC-demethylases is specific for H3K27me3 demethylation (Lu et al., 2008; Luo et al., 2014). EARLY FLOWERING 6 (ELF6/JMJ11) is an activator of *FLC* (Noh et al., 2004), but RELATIVE OF EARLY FLOWERING 6 (REF6/JMJ12) positively regulates *FT* by removing H3K27me3 (Lu et al., 2011). In addition, the H3K27 demethylase REF6 can directly bind to DNA by its own DNA-binding domain (Li et al., 2016a). In this study, we found that WRKY63-activated gene expression in vernalization is associated with decreased H3K27me3 level, suggesting that WRKY63 might be functionally associated with H3K27me3 demethylation to regulate gene expression in *Arabidopsis*. Further studies are needed to investigate the functional association between H3K27me3 demethylases and WRKY63. However, since the removing of H3K27me3 can be directly caused by the transcriptional activation (Holoch et al., 2021), the decreased H3K27me3 might be indirectly caused by the transcriptional activation of WRKY63.

In addition to *COOLAIR* and *COLDAIR*, we found that WRKY63 can also activate the expression of other vernalization-induced genes, such as *CBF1*, *COR47*, *KIN1*, *ADS2*, *AtCP1*, *HD2C*, and *GI*. Intriguingly, the expression of these genes is increased after vernalization. By contrast, *FLC* expression is decreased after vernalization. In addition, WRKY63 can activate *FLC* under non-vernalization conditions. Since there is no difference in the expression of *KIN1*, *ADS2*, *AtCP1*, and *HD2C* between *wrky63* and WT before vernalization treatment, WRKY63 may not affect these genes under non-vernalization conditions. These results support our hypothesis that WRKY63 may associate with different protein complexes to regulate gene expression under vernalization and non-vernalization conditions. Interestingly, WRKY63 functions as a transcriptional activator of *FLC* under non-vernalization condition. However, vernalization increases the binding of WRKY63 to the promoters of the lncRNA *COOLAIR*/*COLDAIR*, resulting in the activation of *COOLAIR*/*COLDAIR* and repression of *FLC* during vernalization. Therefore, WRKY63 acts as a dual regulator that activates *FLC* directly under non-vernalization conditions but represses *FLC* indirectly during vernalization through *COOLAIR*/*COLDAIR*.

According to the GO-BP analysis, we found that the WRKY63 target genes are involved in hormone and stress responses as well as developmental processes, suggesting that in addition to vernalization and flowering regulation, WRKY63 may also be involved in other developmental processes. For example, we found that *CBF1*, *COR47*, and *GI* can be regulated by WRKY63 under both vernalization and non-vernalization conditions. Similar to WRKY63, CBF1, COR47, and GI have also been reported to be involved in drought stress response (Welin et al., 1994; Haake et al., 2002; Riboni et al., 2013). In addition, GI is one of the core regulators in the evening-loop of circadian rhythm and is involved in photoperiod-mediated flowering (Fowler et al., 1999). CBF1 is also regulated by the circadian rhythm and PHYTOCHROME INTERACTING FACTOR 7 (PIF7) (Kidokoro et al., 2009). Further research is required to analyze whether WRKY63 is involved in these processes.

In conclusion, we demonstrated that the transcription factor WRKY63 is involved in the regulation of vernalization-induced flowering. WRKY63 binds to the *FLC* locus and activates the lncRNAs *COOLAIR* and *COLDAIR* under vernalization. Furthermore, WRKY63 can also activate the expression of a subset of vernalization-induced genes and the activation of gene expression mediated by WRKY63 is associated with decreased H3K27me3 (Figure 9).

Materials and methods

Plant materials and growth conditions

In this study, the WT Arabidopsis (*A. thaliana*) Columbia (Col-0) ecotype was used. Plants were grown in growth chambers under 16/8 h light/dark LD or 8/16 h light/dark SD conditions at 22°C. For vernalization treatment, seeds were germinated and grown for 10 days under standard conditions (LD, 22°C), and then transferred to 4°C for 2, 4, or 6 weeks. The *wrky63-2* (*abo3*) mutant (SALK_007496) has the T-DNA insertion in the third exon (Ren et al., 2010), and *wrky63-1* (SALK_068280) has the T-DNA insertion in the promoter region. These *wrky63* mutants were obtained from TAIR (www.arabidopsis.org). The *wrky63*/*ft* and *wrky63*/*flc* mutant plants were generated by crossing *wrky63-2* (*abo3*) with *ft-10* and *flc-3*, respectively. All the above mutants used in this study are in the Col-0 background. *FRI*/*wrky63* mutant plant was generated by crossing *wrky63-2* (*abo3*) with *FRIcol* (Col-0 with a functional *FRI* allele) (Gazzani et al., 2003).

Plasmid construction and plant transformation

The full-length CDS fragments of *WRKY63* were PCR-amplified and cloned into the *pCR8/GW/TOPO* vector

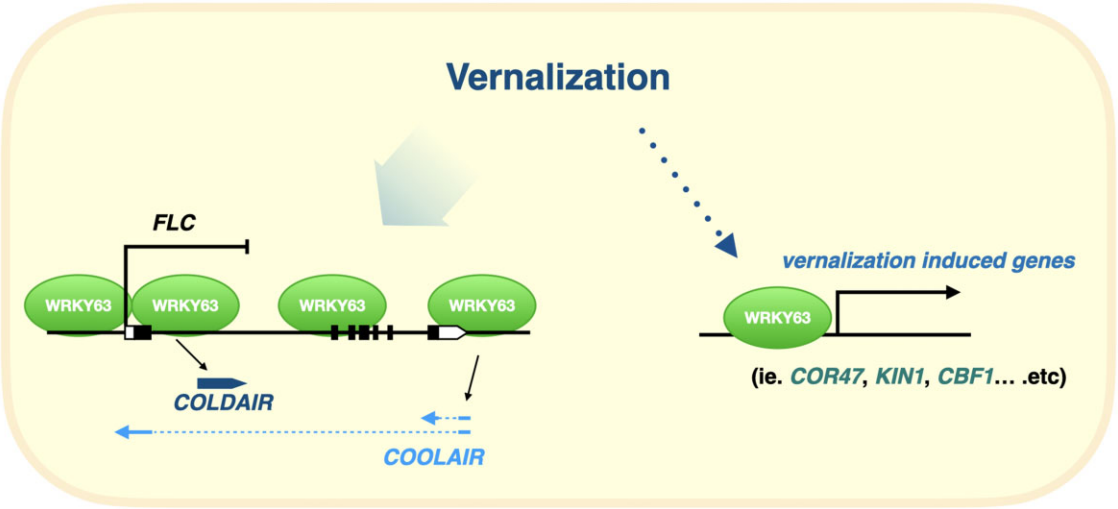

Figure 9 A model of how *Arabidopsis* WRKY63 is involved in vernalization-induced flowering. Without vernalization, WRKY63 can activate *FLC* expression by direct targeting. During vernalization, the binding of WRKY63 is increased in the promoters of the lncRNAs *COOLAIR* and *COLDAIR*, resulting in *COOLAIR* and *COLDAIR* activation. Therefore, the expression of *FLC* is repressed by increased *COOLAIR* and *COLDAIR* during vernalization. Furthermore, WRKY63 can also activate the expression of other vernalization-induced genes.

(Invitrogen). Point mutation constructs were constructed by specific primer sets then cloned into the *pCR8/GW/TOPO* vector (Invitrogen). *WRKY63 was* recombined into the *PK7WGF2* (Invitrogen) to generate the *GFP:WRKY63* plasmid. To construct *WRKY63pro::WRKY63:GFP*, approximately 2-kb promoter with the genome sequence of *WRKY63* was cloned into the *pCR8/GW/TOPO* vector (Invitrogen), then recombined into the *pMDC107* binary vector. The transgenic plants were generated by using the floral dip method.

LUCIFERASE transient assays

The analysis of *LUCIFERASE* transient expression was performed as described previously (Fujimoto et al., 2000; Ohta et al., 2000).The reporter construct [*GAL4BS(4X)-GCC box(4X)-TATA box-Translational enhancer::Firefly LUC*] (Fujimoto et al., 2000; Ohta et al., 2000) contains the binding site (GAL4BS) of the yeast transcription factor GAL4 (Ma and Ptashne, 1987). The effector construct contains the GAL4 DNA binding domain (GAL4-BD) fussed at the N-terminus of WRKY63 (GALBD-WRKY63). GAL4BD was used as a negative control, and GAL4BD fused with the VP16 activation domain (GAL4BD-VP16) (Triezenberg et al., 1988) was used as a positive control. The analyses of *LUCIFERASE* transient expression in protoplasts were described in previous studies (Ohta et al., 2000; Ding et al., 2018). Four micrograms of reporter constructs and 5 μg of effector constructs were used for each co-transfection assays. To analyze the promoter activity of *COOLAIR* and *COLDAIR*, 1.2 kb of *COOLAIR* promoter and 1.5 kb of *COLDAIR* promoter were PCR-amplified, then cloned into the *pCR8/GW/TOPO* vector (Invitrogen). The *COOLAIR* promoter and *COLDAIR* promoter were recombined into *pKGWL7* with the *firefly LUCIFERASE* (*LUC*) as reporter constructs. Effector constructs *35Spro::WRKY63* and *35Spro::mcherry* control were co-transformed as described previously (Ohta et al., 2000; Ding et al., 2018) for transcriptional activity assays. The reporter luciferase activities were standardized by activities of the co-expressed Renilla *LUCIFERASE* (rLUC), and relative reporter activities were calculated. Experiments were repeated at least three times for each reporter–effector combination. Signals of Firefly and Renilla luciferase were assayed with the dual luciferase assay reagents (Promega).

Fluorescence imaging and western blot

The vernalization or non-vernalization treated *WRKY63pro::WRKY63:GFP* transgenic plants were used for the fluorescence imaging. GFP fluorescence was visualized by using the Zeiss Axio Imager.Z2 microscope system (https://www.zeiss.com/microscopy). The GFP signal was quantified in the middle section of cotyledons for analyzing GFP intensity by the Zeiss ZEN software (https://www.zeiss.com/microscopy/int/products/microscope-software/zen.html). GFP fluorescence was observed through the filter sets 46 HE (excitation at 500 nm, beamsplitter at 515 nm, and emission at 535 nm). Images were captured using a 5× objective with tile scan mode. The vernalization and non-vernalization samples were captured in the same field together and then processed and analyzed using the Zeiss ZEN software as described above.

Western blot assays were performed as previously described (Hung et al., 2018). Anti-GFP (Santa Cruz Biotechnologies, catalog no. SC-9996; 1:3,000 dilution), anti-FLAG (sigma, M2; 1:3,000 dilution), and anti-H3 (Abcam, ab1791; 1:3,000 dilution) antibodies were used as primary antibodies for Western blot; the resulting signals were detected by using an Advansta ECL Western blotting kit (Advansta, K-12045-D20).

Reverse transcription quantitative PCR analysis

Total RNA was isolated using TRIZOL reagent (Invitrogen, 15596026) according to the manufacturer's instructions. Two micrograms of DNAse (Promega, RQ1 #M6101) treated total RNA were used to synthesize cDNA (Promega, #1012891). RT-qPCR was performed using iQ SYBR Green Supermix solution (Bio-Rad, #170-8880). The CFX96 Real-Time PCR Detection System (Bio-Rad Laboratories, Inc.) was used with the following cycling conditions: 95°C for 10 min, followed by 45 cycles of 95°C for 15 s, 60°C for 30s, and then fluorescent detection. This was immediately followed by a melting curve (65°C–95°C, incrementing 0.5°C for 5 s, and plate reading). The melting curve analysis confirmed the absence of non-specific products. Each sample was quantified at least in triplicate and normalized by calculating delta Cq (quantification cycle) to the expression of the internal control *Ubiquitin10* (*UBQ10*). The Cq and relative expression level are calculated by the Biorad CFX Manager 3.1 based on the MIQE guidelines. Standard deviations represent at least three technical and two biological replicates. The variance in average data is represented by standard error of the mean (SEM). The standard deviation (SD), SEM determination, and *P*-value were calculated using Student's paired *t* test. The gene-specific primers used for RT-qPCR are listed in Supplemental Table S1.

Chromatin immunoprecipitation assays

ChIP assays were performed as previously described (Hung et al., 2018, 2021). Chromatin extracts were prepared from seedlings treated with 1% formaldehyde (v/v). The chromatin was sheared to the mean length of 500 bp by sonication, proteins and DNA fragments were then immunoprecipitated using antibodies against GFP (Abcam, catalog no. ab290), H3K27me3 (Diagenode, catalog no. C15410195), or H3Ac (Millipore, catalog no. 06-599). The DNA cross-linked to immunoprecipitated proteins were reversed and then analyzed by qPCR using specific primers (Supplemental Table S1). Percent input was calculated as follows: 2∧(Cq(IN)-Cq(IP))X100. Cq is the quantification cycle as calculated by the Biorad CFX Manager 3.1 based on the MIQE guidelines. Standard deviations represent at least three technical and two biological replicates. The variance in average data is represented by SEM . The SD, SEM determination, and *P*-value were calculated using Student's paired *t* test.

ChIP-seq and data analyses

ChIP-seq assays were performed based on previous research (Hung et al., 2018, 2021). Two nanograms of DNA from ChIP was pooled to ensure that there are enough starting DNA for library construction. Two biological replicates were prepared and sequenced for each ChIP-seq experiment. The ChIP DNA was first tested by RT-qPCR and then used to prepare ChIP-seq libraries. End repair, adaptor ligation, and amplification were carried out using the NEBNext Ultra II DNA Library Prep kit (cat no. E7103) according to the manufacturer's protocol. The Novoseq PE150 was used for high-throughput sequencing of the ChIP-seq libraries. The raw sequence data were processed using the GAPipeline Illumina sequence data analysis pipeline. Reads were mapped to the TAIR10 *Arabidopsis* genome (Lamesch et al., 2012) using Qiagen CLC Genomics Workbench (https://www.qiagenbioinformatics.com) with default settings. Reads that mapped to multiple regions were discarded. The data were then imported into the Integrated Genome Viewer (IGV) (Thorvaldsdottir et al., 2013) for visualization. The distribution of the ChIP binding peaks was analyzed with ChIPseeker (Yu et al., 2015), and a high-read random *Arabidopsis* genomic region subset (1,350,000 regions) was used to represent the ratio of the total *Arabidopsis* genomic regions. The regions with peak value less than 15 were excluded to locate the target genes (Supplemental Table S2). To identify DNA motifs enriched sites, 400-bp sequences encompassing each peak summit (200-bp upstream and 200-bp downstream) were extracted and searched for enriched DNA motifs using MEME-ChIP with the default parameters (Machanick and Bailey, 2011). To compare the association between RNA expression and histone modifications, the ChIP-seq results as well as previously published *Arabidopsis* RNA-seq (GSE123459), H3K27me3 (GSE130291), and Pol II (GSE95301) ChIP-seq data (Gibbs et al., 2018; Liu et al., 2018; Xi et al., 2020) were analyzed by using deepTools. The WRKY63 ChIP-seq short read data have been submitted to the NCBI Gene Expression Omnibus (GEO) database (GSE177884).

Accession numbers

Sequence data from this article can be found in the GenBank/EMBL data libraries under accession numbers (Supplemental Table S1). Short read data of WRKY63 ChIP-seq have been submitted to the NCBI-Gene Expression Omnibus (GEO) database (GSE177884).

Supplemental data

The following materials are available in the online version of this article.

Supplemental Figure S1. Identification of *wrky63* T-DNA insertion mutants.

Supplemental Figure S2. Flowering phenotypes of WT, *wrky63*, *ft* and *wrky 63 ft*.

Supplemental Figure S3. Flowering phenotypes of WT, *wrky63*, *flc* and *wrky63 flc*.

Supplemental Figure S4. Flowering time of *35Spro::GFP:WRKY63* and *pro::WRKY63:GFP* transgenic plants.

Supplemental Figure S5. The flowering phenotype of WT, *wrky63-1* and *wrky63-2* under vernalization in LD.

Supplemental Figure S6. The protein accumulation of WRKY63 is induced by vernalization.

Supplemental Figure S7. The flowering phenotype and gene expression patterns of *FRIcol* and *FRI/wrky63*.

Supplemental Figure S8. H3Ac level on the *FLC* locus *in vivo*.

Supplemental Figure S9. Gene Ontology Biological Processes (GO-BP) analysis of WRKY63 targeted genes.

Supplemental Figure S10. WRKY63 is associated with vernalization-induced gene activation and demethylation of H3K27me3.

Supplemental Table S1. Primers used in this study and the gene accession numbers.

Supplemental Table S2. ChIP-seq data of WRKY63 targeted genes.

Acknowledgments

We thank Technology Commons, College of Life Science, National Taiwan University for the convenient use of the Zeiss Axio Imager.Z2 microscope system and Bio-Rad real-time PCR system. We also thank to Pei-Yin, Wu in Technology Commons for technical support.

Funding

This work was supported by the Ministry of Science and Technology of the Republic of China (108-2311-B-002-013-MY3 and 110-2311-B-002-027 to K.W.) and National Taiwan University (NTUCC-111L893001 to K.W.).

Conflict of interest statement. None declared.

References

Bardou F, Ariel F, Simpson CG, Romero-Barrios N, Laporte P, Balzergue S, Brown JWS, Crespi M (2014) Long noncoding RNA modulates alternative splicing regulators in *Arabidopsis*. Dev Cell **30**: 166–176

Birkenbihl RP, Kracher B, Roccaro M, Somssich IE (2017) Induced genome-wide binding of three *Arabidopsis* WRKY transcription factors during early MAMP-triggered immunity. Plant Cell **29**: 20–38

Chen MJ, Thelen JJ (2013) ACYL-LIPID DESATURASE2 is required for chilling and freezing tolerance in *Arabidopsis*. Plant Cell **25**: 1430–1444

De Lucia F, Crevillen P, Jones AM, Greb T, Dean C (2008) A PHD-polycomb repressive complex 2 triggers the epigenetic silencing of FLC during vernalization. Proc Natl Acad Sci USA **105**: 16831–16836

Delk NA, Johnson KA, Chowdhury NI, Braam J (2005) CML24, regulated in expression by diverse stimuli, encodes a potential Ca2 + sensor that functions in responses to abscisic acid, daylength, and ion stress. Plant Physiol **139**: 240–253

Ding Y, Sun T, Ao K, Peng Y, Zhang Y, Li X, Zhang Y (2018) Opposite roles of salicylic acid receptors NPR1 and NPR3/NPR4 in transcriptional regulation of plant immunity. Cell **173**: 1454–1467 e1415

Eulgem T, Rushton PJ, Robatzek S, Somssich IE (2000) The WRKY superfamily of plant transcription factors. Trends Plant Sci **5**: 199–206

Fornara F, de Montaigu A, Sanchez-Villarreal A, Takahashi Y, van Themaat EVL, Huettel B, Davis SJ, Coupland G (2015) The GI-CDF module of *Arabidopsis* affects freezing tolerance and growth as well as flowering. Plant J **81**: 695–706

Fowler S, Lee K, Onouchi H, Samach A, Richardson K, Morris B, Coupland G, Putterill J (1999) GIGANTEA: A circadian clock-controlled gene that regulates photoperiodic flowering in *Arabidopsis* and encodes a protein with several possible membrane-spanning domains. EMBO J **18**: 4679–4688

Fujimoto SY, Ohta M, Usui A, Shinshi H, Ohme-Takagi M (2000) *Arabidopsis* ethylene-responsive element binding factors act as transcriptional activators or repressors of GCC box-mediated gene expression. Plant Cell **12**: 393–404

Gazzani S, Gendall AR, Lister C, Dean C (2003) Analysis of the molecular basis of flowering time variation in *Arabidopsis* accessions. Plant Physiol **132**: 1107–1114

Gendall AR, Levy YY, Wilson A, Dean C (2001) The VERNALIZATION 2 gene mediates the epigenetic regulation of vernalization in *Arabidopsis*. Cell **107**: 525–535

Gibbs DJ, Tedds HM, Labandera AM, Bailey M, White MD, Hartman S, Sprigg C, Mogg SL, Osborne R, Dambire C, et al. (2018) Oxygen-dependent proteolysis regulates the stability of angiosperm polycomb repressive complex 2 subunit VERNALIZATION 2. Nat Commun **9**(1): 5438

Guo WW, Ward RW, Thomashow MF (1992) Characterization of a cold-regulated wheat gene related to *Arabidopsis* Cor47. Plant Physiol **100**: 915–922

Haake V, Cook D, Riechmann JL, Pineda O, Thomashow MF, Zhang JZ (2002) Transcription factor CBF4 is a regulator of drought adaptation in *Arabidopsis*. Plant Physiol **130**: 639–648

Heo JB, Sung S (2011) Vernalization-mediated epigenetic silencing by a long intronic noncoding RNA. Science **331**: 76–79

Hepworth J, Dean C (2015) Flowering locus C's lessons: Conserved chromatin switches underpinning developmental timing and adaptation. Plant Physiol **168**: 1237–1245

Hepworth SR, Valverde F, Ravenscroft D, Mouradov A, Coupland G (2002) Antagonistic regulation of flowering-time gene *SOC1* by CONSTANS and FLC via separate promoter motifs. EMBO J **21**: 4327–4337

Holoch D, Wassef M, Lovkvist C, Zielinski D, Aflaki S, Lombard B, Hery T, Loew D, Howard M, Margueron R (2021) A cis-acting mechanism mediates transcriptional memory at Polycomb target genes in mammals. Nat Genet **53**: 1686–1697

Hu XY, Kong XX, Wang CT, Ma L, Zhao JJ, Wei JJ, Zhang XM, Loake GJ, Zhang TC, Huang JL, et al. (2014) Proteasome-mediated degradation of FRIGIDA modulates flowering time in *Arabidopsis* during vernalization. Plant Cell **26**: 4763–4781

Hung FY, Chen C, Yen MR, Hsieh JWA, Li CL, Shih YH, Chen FF, Chen PY, Cui YH, Wu KQ (2020a) The expression of long non-coding RNAs is associated with H3Ac and H3K4me2 changes regulated by the HDA6-LDL1/2 histone modification complex in Arabidopsis. NAR Genom Bioinform **2**(3): lqaa066

Hung FY, Chen FF, Li CL, Chen C., Lai YC, Chen JH, Cui YH, Wu KQ (2018) The *Arabidopsis* LDL1/2-HDA6 histone modification complex is functionally associated with CCA1/LHY in regulation of circadian clock genes. Nucleic Acids Res **46**: 10669–10681

Hung FY, Chen JH, Feng YR, Lai YC, Yang SG, Wu KQ (2020b) *Arabidopsis* JMJ29 is involved in trichome development by regulating the core trichome initiation gene GLABRA3. Plant J **103**: 1735–1743

Hung FY, Lai YC, Wang J, Feng YR, Shih YH, Chen JH, Sun HC, Yang S, Li C, Wu K (2021) The *Arabidopsis* histone demethylase JMJ28 regulates *CONSTANS* by interacting with FBH transcription factors. Plant Cell **33**(4): 1196–1211

Kalde M, Barth M, Somssich IE, Lippok B (2003) Members of the *Arabidopsis* WRKY group III transcription factors are part of different plant defense signaling pathways. Mol Plant Microbe Interact **16**(4): 295–305

Kidokoro S, Maruyama K, Nakashima K, Imura Y, Narusaka Y, Shinwari ZK, Osakabe Y, Fujita Y, Mizoi J, Shinozaki K, et al. (2009) The phytochrome-interacting factor PIF7 negatively regulates *DREB1* expression under circadian control in *Arabidopsis*. Plant Physiol **151**: 2046–2057

Kim DH, Sung S (2013) Coordination of the vernalization response through a VIN3 and *FLC* gene family regulatory network in *Arabidopsis*. Plant Cell **25**: 454–469

Kim DH, Xi Y, Sung S (2017) Modular function of long noncoding RNA, *COLDAIR*, in the vernalization response. PLoS Genet **13**: e1006939

Knight H, Trewavas AJ, Knight MR (1996) Cold calcium signaling in *Arabidopsis* involves two cellular pools and a change in calcium signature after acclimation. Plant Cell **8**: 489–503

Lamesch P, Berardini TZ, Li DH, Swarbreck D, Wilks C, Sasidharan R, Muller R, Dreher K, Alexander DL, Garcia-Hernandez M, et al. (2012) The *Arabidopsis* Information Resource (TAIR): Improved gene annotation and new tools. Nucleic Acids Res **40**: D1202–D1210

Li CL, Gu LF, Gao L, Chen C, Wei CQ, Qiu Q, Chien CW, Wang SK, Jiang LH, Ai LF, et al. (2016a) Concerted genomic targeting of H3K27 demethylase REF6 and chromatin-remodeling ATPase BRM in *Arabidopsis*. Nat Genet **48**(6): 687–693

Li W, Wang HP, Yu DQ (2016b) Arabidopsis WRKY transcription factors WRKY12 and WRKY13 oppositely regulate flowering under short-day conditions. Mol Plant **9**: 1492–1503

Lim CJ, Park J, Shen M, Park HJ, Cheong MS, Park KS, Baek D, Bae MJ, Ali A, Jan M, et al. (2020) The histone-modifying complex PWR/HOS15/HD2C epigenetically regulates cold tolerance. Plant Physiol **184**: 1097–1111

Liu C, Xin Y, Xu L, Cai ZK, Xue YC, Liu Y, Xie DX, Liu YL, Qi YJ (2018) Arabidopsis ARGONAUTE 1 binds chromatin to promote gene transcription in response to hormones and stresses. Dev Cell **44**(3): 348–361

Liu X, Hao LL, Li DY, Zhu LH, Hu SN (2015) Long non-coding RNAs and their biological roles in plants. Genom Proteom Bioinf **13**: 137–147

Llorca CM, Potschin M, Zentgraf U (2014) bZIPs and WRKYs: Two large transcription factor families executing two different functional strategies. Front Plant Sci **5**: 169

Lu FL, Cui X, Zhang SB, Jenuwein T, Cao XF (2011) *Arabidopsis* REF6 is a histone H3 lysine 27 demethylase. Nat Genet **43**: 715–719

Lu FL, Li GL, Cui X, Liu CY, Wang XJ, Cao XF (2008) Comparative analysis of JmjC domain-containing proteins reveals the potential histone demethylases in Arabidopsis and rice. J Integr Plant Biol **50**: 886–896

Luo M, Hung FY, Yang SG, Liu XC, Wu KQ (2014) Histone lysine demethylases and their functions in plants. Plant Mol Biol Rep **32**: 558–565

Ma J, Ptashne M (1987) Deletion analysis of GAL4 defines two transcriptional activating segments. Cell **48**: 847–853

Machanick P, Bailey TL (2011) MEME-ChIP: Motif analysis of large DNA datasets. Bioinformatics **27**: 1696–1697

Maeo K, Hayashi S, Kojima-Suzuki H, Morikami A, Nakamura K (2001) Role of conserved residues of the WRKY domain in the DNA-binding of tobacco WRKY family proteins. Biosci Biotech Biochem **65**: 2428–2436

Marquardt S, Raitskin O, Wu Z, Liu F, Sun Q, Dean C (2014) Functional consequences of splicing of the antisense transcript *COOLAIR* on *FLC* transcription. Mol Cell **54**: 156–165

Michaels SD, Amasino RM (2001) Loss of FLOWERING LOCUS C activity eliminates the late-flowering phenotype of FRIGIDA and autonomous pathway mutations but not responsiveness to vernalization. Plant Cell **13**: 935–941

Noh B, Lee SH, Kim HJ, Yi G, Shin EA, Lee M, Jung KJ, Doyle MR, Amasino RM, Noh YS (2004) Divergent roles of a pair of homologous jumonji/zinc-finger-class transcription factor proteins in the regulation of *Arabidopsis* flowering time. Plant Cell **16**: 2601–2613

Ohta M, Ohme-Takagi M, Shinshi H (2000) Three ethylene-responsive transcription factors in tobacco with distinct transactivation functions. Plant J **22**: 29–38

Park J, Lim, CJ, Shen MZ, Park HJ, Cha JY, Iniesto E, Rubio V, Mengiste T, Zhu JK, Bressan RA, et al. (2018) Epigenetic switch from repressive to permissive chromatin in response to cold stress. Proc Natl Acad Sci USA **115**: E5400–E5409

Ren XZ, Chen ZZ, Liu Y, Zhang HR, Zhang M, Liu QA, Hong XH, Zhu JK, Gong ZZ (2010) ABO3, a WRKY transcription factor, mediates plant responses to abscisic acid and drought tolerance in *Arabidopsis*. Plant J **63**: 417–429

Riboni M, Galbiati M, Tonelli C, Conti L (2013) GIGANTEA enables drought escape response via abscisic acid-dependent activation of the florigens and *SUPPRESSOR OF OVEREXPRESSION OF CONSTANS*. Plant Physiol **162**: 1706–1719

Rushton PJ, Macdonald H, Huttly AK, Lazarus CM, Hooley R (1995) Members of a new family of DNA-binding proteins bind to a conserved cis-element in the promoters of alpha-Amy2 genes. Plant Mol Biol **29**: 691–702

Rushton PJ, Somssich IE, Ringler P, Shen QJ (2010) WRKY transcription factors. Trends Plant Sci **15**: 247–258

Searle I, He Y, Turck F, Vincent C, Fornara F, Krober S, Amasino RA, Coupland G (2006) The transcription factor FLC confers a flowering response to vernalization by repressing meristem competence and systemic signaling in *Arabidopsis*. Genes Dev **20**: 898–912

Stockinger EJ, Gilmour SJ, Thomashow MF (1997) *Arabidopsis thaliana* CBF1 encodes an AP2 domain-containing transcriptional activator that binds to the C-repeat/DRE, a cis-acting DNA regulatory element that stimulates transcription in response to low temperature and water deficit. Proc Natl Acad Sci USA **94**: 1035–1040

Sun QW, Csorba T, Skourti-Stathaki K, Proudfoot NJ, Dean C (2013) R-loop stabilization represses antisense transcription at the *Arabidopsis FLC* locus. Science **340**: 619–621

Swiezewski S, Liu F, Magusin A, Dean C (2009) Cold-induced silencing by long antisense transcripts of an *Arabidopsis* Polycomb target. Nature **462**: 799–802

Thorvaldsdottir H, Robinson JT, Mesirov JP (2013) Integrative genomics viewer (IGV): High-performance genomics data visualization and exploration. Brief Bioinform **14**: 178–192

Triezenberg SJ, Kingsbury, RC, McKnight SL (1988) Functional dissection of VP16, the trans-activator of herpes simplex virus immediate early gene expression. Genes Dev **2**: 718–729

Van Aken O, Zhang BT, Law S, Narsai R, Whelan J (2013) AtWRKY40 and AtWRKY63 modulate the expression of stress-responsive nuclear genes encoding mitochondrial and chloroplast proteins. Plant Physiol **162**: 254–271

Wang KC, Yang YW, Liu B, Sanyal A, Corces-Zimmerman R, Chen Y, Lajoie BR, Protacio A, Flynn RA, Gupta RA, et al. (2011) A long noncoding RNA maintains active chromatin to coordinate homeotic gene expression. Nature **472**: 120–124

Welin BV, Olson A, Nylander M, Palva ET (1994) Characterization and differential expression of dhn/lea/rab-like genes during cold acclimation and drought stress in *Arabidopsis thaliana*. Plant Mol Biol **26**: 131–144

Wood CC, Robertson M, Tanner G, Peacock WJ, Dennis ES, Helliwell CA (2006) The *Arabidopsis thaliana* vernalization response requires a polycomb-like protein complex that also includes VERNALIZATION INSENSITIVE 3. Proc Natl Acad Sci USA **103**: 14631–14636

Xi Y, Park SR, Kim DH, Kim ED, Sung S (2020) Transcriptome and epigenome analyses of vernalization in *Arabidopsis thaliana*. Plant J **103**: 1490–1502

Yu GC, Wang LG, He QY (2015) ChIPseeker: An R/Bioconductor package for ChIP peak annotation, comparison and visualization. Bioinformatics **31**: 2382–2383

Yu YC, Liu ZH, Wang L, Kim SG, Seo PJ, Qiao M, Wang N, Li S, Cao XF, Park CM, et al. (2016) WRKY71 accelerates flowering via the direct activation of *FLOWERING LOCUS T* and *LEAFY* in *Arabidopsis thaliana*. Plant J **85**: 96–106

Zhang LP, Chen LG, Yu DQ (2018) Transcription factor WRKY75 interacts with DELLA proteins to affect flowering. Plant Physiol **176**: 790–803